Theoret. chim. Acta (Berl.) 30, 137—150 (1973)
© by Springer-Verlag 1973

Electron Redistribution in Disulfide Bonds under Torsion

Donald B. Boyd
The Lilly Research Laboratories, Indianapolis, USA

Received February 8, 1973

The origin of the conformational preference of acyclic disulfides is elucidated with population analyses and electron density maps of extended Hückel wave functions for HSSH and H_3CSSCH_3. Overlap population between the sulfurs is greatest when the dihedral angle about the S–S bond is near 90° because the negative contributions from the repulsive interactions of the lone-pair electrons are minimized in this conformation. Electron density maps are introduced to illustrate the rearrangement of the valence electrons in HSSH when the molecule is formed from the isolated atoms and the redistribution which occurs when the molecule is twisted about the S–S bond. A "*C*"-shaped distribution is found for the lone-pair clouds around each sulfur. The spacing between these clouds and the transfer of density away from the sulfurs toward the hydrogens are enhanced when the dihedral angle is near 90°.

Key words: Hydrogen persulfide – Disulfides, conformation of

Introduction

Recently, we have shown that the extended Hückel molecular orbital (EH MO) method can be used to explain the relation of the *uv* absorption spectra of organic disulfides to the dihedral angle about the S–S bond [1]. Computed transition energies and oscillator strengths varied in a manner qualitatively consistent with experiment for several of the long wavelength bands through the range of observed dihedral angles ($\sim 0°$ to $\sim 120°$). Since the EH MO's appear to give a satisfactory description of the electronic structure of the disulfide chromophore, we wish to bring them to bear on another aspect of disulfides, namely, the origin of the roughly 90° preference for the dihedral angle about the S–S bond. For instance, in HSSH the dihedral angle [2] is 90.6°, and in H_3CSSCH_3, the CSSC angle [3, 4] is about 85°. Of course, bulky substituents [1] can force the dihedral angle to open beyond 90°, and small rings or intramolecular hydrogen bonds [1] can impose dihedral angles considerably smaller than 90°.

Calculations by the EH method were carried out using previously published parameter values [5–7]. The usual Slater-type basis sets were employed, including the S 3*d* functions. Hydrogen persulfide, HSSH, and dimethyldisulfide, H_3CSSCH_3, were assigned dihedral angles from 0° (*cis*) to 180° (*trans*), including the experimental values near 90°. Bond lengths and angles were held fixed at the microwave determined values [2, 3]. For purposes of computing potential energy curves for internal rotation, $0.5\,\Sigma\varepsilon_i$ was employed. This quantity has

Table 1. Calculations on the barriers to internal rotation in HSSH

Method	Preferred dihedral angle	*cis* barrier (kcal/mole)	*trans* barrier (kcal/mole)	Ref.
Simple LCAO-MO	90°	6–14	–	[18]
CNDO with Sichel-Whitehead parameters	90°	2.7	2.7	[19]
CNDO with Santry-Segal parameters	95°	3.4	0.8	[17]
Ab initio with Gaussian-type functions (Total energy: −792.66 a.u.)	90–100°	7.4	1.9	[15]
Ab initio with Gaussian-type functions (Total energy: −793.97 a.u.)	98°	7.7	2.2	[17]
Ab initio with Gaussian-type functions (Total energy: −796.18 a.u.)	91°	9.3	6.0	[16]
Present work	80–90°	1.5	0.9	

been shown [8, 9] to be more appropriate for evaluating total energies of molecules in EH theory than the simple sum of the eigenvalues of the occupied MO's over all valence electrons, $\Sigma\varepsilon_i$.

The main purpose of this paper is to use electron density maps for extending our understanding of the disulfide rotational barriers and for visualizing the shape of the electron lone-pair clouds on sulfur. Electron density maps of EH MO's have been established as a highly useful technique in the study of molecular electronic structures [6, 9–13]. Before presenting the illustrations, Mulliken [14] population analyses will be done on both HSSH and H_3CSSCH_3. Our population analysis results are presented in more detail than has been done by previous authors, so that all aspects of the variation of bond strengths and orbital populations can be traced as a function of dihedral angle. We will see that the essential features of the population analyses, which have been observed in *ab initio* calculations [15–17], are also displayed by our semi-empirical EH MO's. Hence the EH MO electron density maps should further elucidate the electron redistribution accompanying the conformational changes in the disulfide group. Electron density difference maps computed by standard procedures [13] will be presented for the smaller model compound HSSH.

Barriers to Internal Rotation in HSSH and H_3CSSCH_3

As with numerous other quantum mechanical studies [15–19], our EH calculations give the correct general shape for the potential energy curve of HSSH (Table 1). But the EH barrier heights are obviously low compared to the *ab initio* values. Experimentally, the heights are not yet known precisely. The EH calculations do mimic the *ab initio* calculations [15–17] in regard to the S–S overlap population, n(S–S), being greatest when the dihedral angle is 90°. The value of n(S–S) increases from 0.831 at a dihedral angle of 0° to 0.854 at 90°, and then drops to 0.844 at 180°. A significant property of n(S–S) can be found by

breaking it down into σ and π components. Whereas the σ overlap population between the sulfurs increases monotonically as the dihedral angle is opened from 0–180°, the π value peaks near 90° at 0.178, compared to 0.162 at 0° and 180°. It follows that the interactions of valence AO's of π symmetry with respect to the S–S axis determine the preferred 90° conformation in disulfides. Furthermore, a repulsive interaction exists between the lone-pair electrons of each sulfur: the $S_1 3p_\pi - S_2 3p_\pi$ contribution to the π component of n(S–S) is negative. It is mainly due to the $3p_\pi - 3d_\pi$ interactions that a net positive π component is obtained in our calculations. The $S_1 3p_\pi - S_2 3p_\pi$ overlap contribution is least negative when the dihedral angle is near 90°, thus indicating that the repulsion between the lone-pair electrons is somewhat relieved in this conformation. The population analysis of the EH MO's also gives the smallest charge separation between S and H at this geometry: the net charge on sulfur, Q(S), is −0.098 at 0°, −0.087 at 90°, and −0.092 at 180°.

Other quantities in the population analysis of HSSH did not show extrema at 90°. For instance, the S–H overlap population decreased marginally and monotonically from 0.761 at 0° to 0.756 at 180°. The only *ab initio* calculations [15] to report n(S–H) give a shallow minimum near 90°. The total occupation of the 3*d* AO's on each sulfur increased steadily from 0.101 *e* at 0° to 0.115 *e* at 180°. Thus, the 3*d* AO's are not greatly occupied in the ground state of HSSH, and, in fact, the extent of occupation is almost the same as in the large basis set *ab initio* calculations [16]. At a dihedral angle of 90°, the rigorous dipole moment computed from all one- and two-center integrals [20] is 2.87 *D*. This contains a contribution of 0.79 *D* from the net atomic charges and a contribution of 3.88 *D* from each sulfur atomic dipole moment [13, 20]. The latter quantity reflects the large asymmetrical polarization of charge due to the lone-pair electrons as will be displayed later. A rather old experimental [21] dipole moment of 1.18 *D* for HSSH is bracketed by our rigorous and point charge values. The rigorous dipole moment of the hypothetical *cis* planar conformer of HSSH is 4.12 *D*.

In dimethyldisulfide H_3CSSCH_3, there are two S–C bonds and one S–S bond about which hindered rotation takes place. Calculations were done through the range of CSSC dihedral angles with three different methyl group arrangements as graphed in Fig. 1. The most stable geometry has a dihedral angle of about 90° and both methyls staggered. When the methyls are in their equilibrium conformation, the *cis* barrier for the S–S bond is 7.0 kcal/mole, and the *trans* barrier is 2.2 kcal/mole. The rotational barrier about the S–C bonds can be seen in Fig. 1 to be about 1.2 kcal/mole at those CSSC dihedral angles large enough to avoid steric hindrance between the methyl hydrogens. Thus, the predicted equilibrium conformation and the various barrier heights are in good agreement with experiment [3, 4, 18, 22]. Of the several previous calculations on the conformational energy of H_3CSSCH_3, the PCILO method [23] yielded a preferred dihedral angle of 100°, a *cis* barrier of 2.9 kcal/mole, and a *trans* barrier of 1.3 kcal/mole. One point about the PCILO calculations is that the molecule at a dihedral angle of 100° is predicted to be 1 kcal/mole more stable when both methyls are eclipsed than when both methyls are staggered. On the other hand, the EH calculations agree with

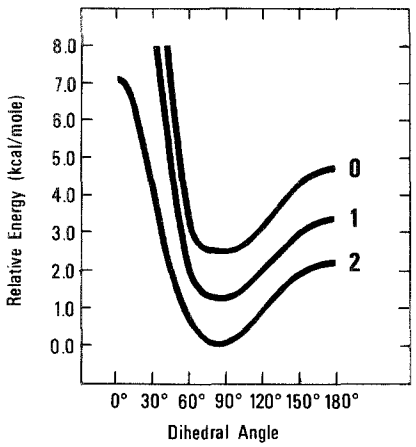

Fig. 1. Conformational energies of H_3CSSCH_3 with both methyls staggered (2), one methyl staggered and one eclipsed (1), and both methyls eclipsed (0) with respect to the S–S bond. The energy is relative to that for the most stable conformation. The top two curves extend off the graph at small dihedral angles because of steric hindrance between hydrogens of each methyl group

experiment [4] by favoring a staggered arrangement for the methyl groups. Perahia and Pullman [23] refer to some work [24] where an EH method failed to give the correct shape of the potential energy curve for H_3CSSCH_3. Instead of the near 90° dihedral angle, a 180° angle was predicted to be most stable. However, we encountered no difficulty in the implementation of our EH method. Other calculations on dimethyldisulfide used a ZDO–SCF method [25] and showed the total energy to be lower at 90° than at smaller dihedral angles, but the barrier heights of 45.9 kcal/mole (*cis*) and 14.5 kcal/mole (*trans*) seem much too high.

The Mulliken population analyses of the most stable conformers of H_3CSSCH_3 yield conclusions similar to those for HSSH. The overlap population of the S–S bond maximizes at 0.952 and the charge on sulfur, Q(S), becomes least negative at -0.038 when the CSSC dihedral angle is 90°. The overlap population of the S–C bonds reaches a peak of 0.675 and Q(C) becomes most negative (-0.119) when the dihedral angle is around 60°. The rigorous dipole moment of H_3CSSCH_3 with both methyls staggered decreases monotonically from 5.70 *D* in the *cis* conformation to zero in the *trans*. At a dihedral angle of 90°, our rigorous dipole moment of 3.91 *D* and point charge value of 0.82 *D* again bracket the experimental value [3] of 1.985 *D*.

Electron Density Maps of HSSH

We did not have the benefit of a plotter in the preparation of the electron density maps seen in Figs. 2–10. Hence our figures are made by photographing printed output from the computer (IBM 360/65). Our computer program can take a two-dimensional array of numbers, such as electron densities, and find specified contours of equal density. The resolution of the printout is limited by the size and ratio of height to width of the type characters. However, any area

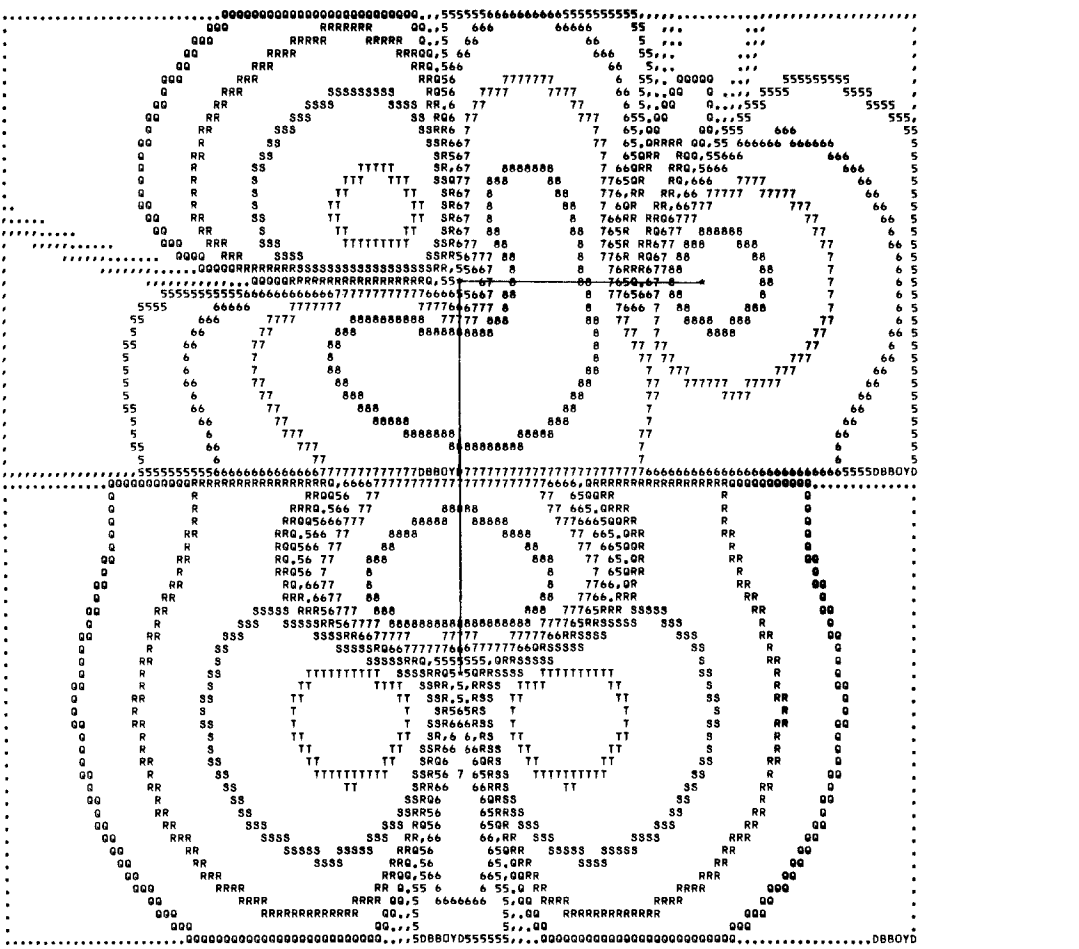

Fig. 2. Electron density in the 0° conformer of HSSH. The difference between the molecular and the spherically symmetric, ground state atomic densities is plotted in two mutually perpendicular planes through the S–S bond: the upper half shows the density in the plane of the S–S–H atoms; the lower half shows the density perpendicular to the S–S–H plane at the other end of the molecule. Each half of the figure, which splits the molecule at the midpoint of the S–S bond, covers 5 × 2.5 Å. Because of the C_{2V} symmetry of the *cis* conformer, both halves of the molecule are equivalent

of the molecule may be magnified as much as necessary by having many maps each covering a small portion. The scale used in our figures was selected on the basis of giving maximum magnification of the molecule while still allowing the contour characters to be legible. Numerical characters correspond to negative density differences, i.e., a deficiency of electrons, and alphabetic characters correspond to positive density differences, i.e., an excess of electrons. Magnitudes of the density corresponding to each character are 0.00024 e/bohr^3 for 5 or Q, 0.00112 for 6 or R, 0.0056 for 7 or S, 0.0280 for 8 or T, and 0.1400 for 9 or U. Nodes occur in the middle of the dotted (.,) contours. Some contours appear to be discontinuous in areas of steep changes in density because of the limited resolution. Internuclear axes between bonded atoms are drawn by solid lines if the atoms

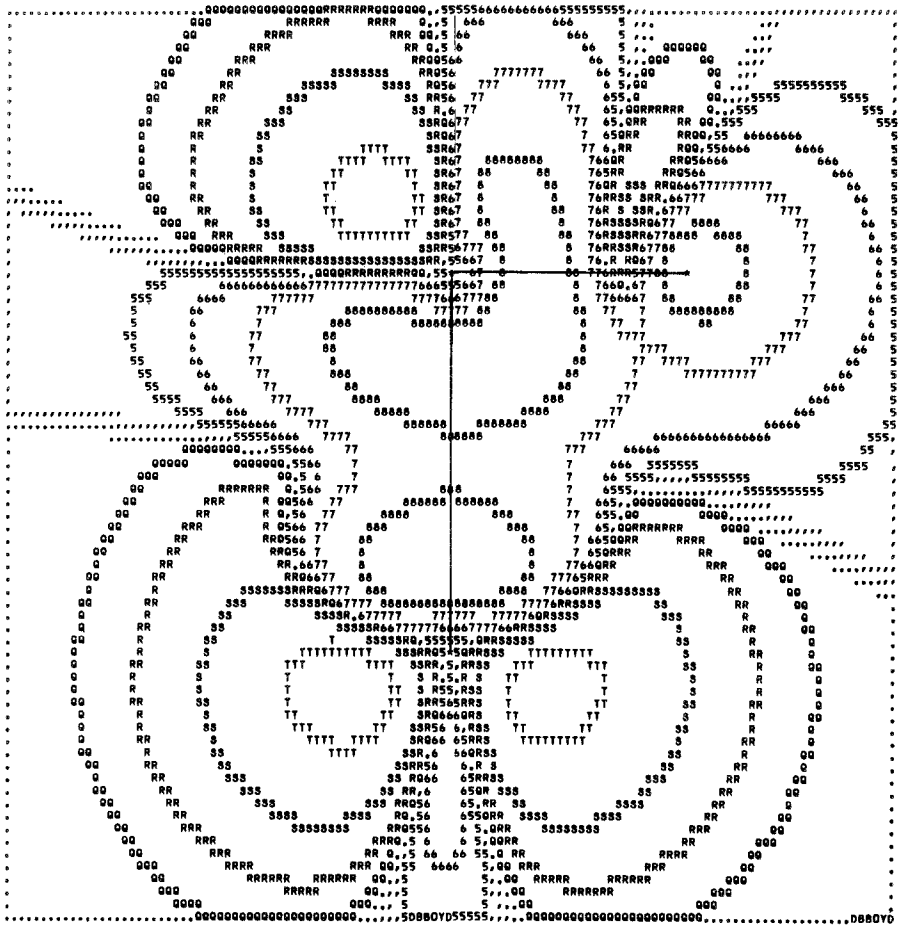

Fig. 3. Electron density in the 90° conformer of HSSH. The map covers 5 × 5 Å and shows the difference in molecular and atomic densities in the S–S–H plane

lie in the plane of calculation and by dashed lines otherwise. Density maps of the *trans* planar conformer of HSSH show no interesting differences from those for the *cis* planar conformer, except for the flip at one end of the molecule. Consequently, in order to conserve journal space, only plots of the conformers with dihedral angles of 0° and 90° are included here.

By mentally assembling the various slices through the molecule (Figs. 2–7), one ascertains that the regions occupied by the lone-pair electrons near each sulfur are roughly "*C*"-shaped. The plane of the "*C*" is perpendicular to the S–S–H plane at each end of the molecule with the top and bottom of the "*C*" above and below the sulfur nucleus. There is more electron density near the ends of the "*C*" than in the mid-section, which means that the lone-pair regions are intermediate between the directed valence implied by sp^3 hybrid orbitals and a uniform, quasi-spherical distribution. Imagining that the "*C*" is hinged on the sulfur, one observes that the "*C*" is swiveled away from the other sulfur. This swiveling to behind the plane of Figs. 5–7 means that the effective distance

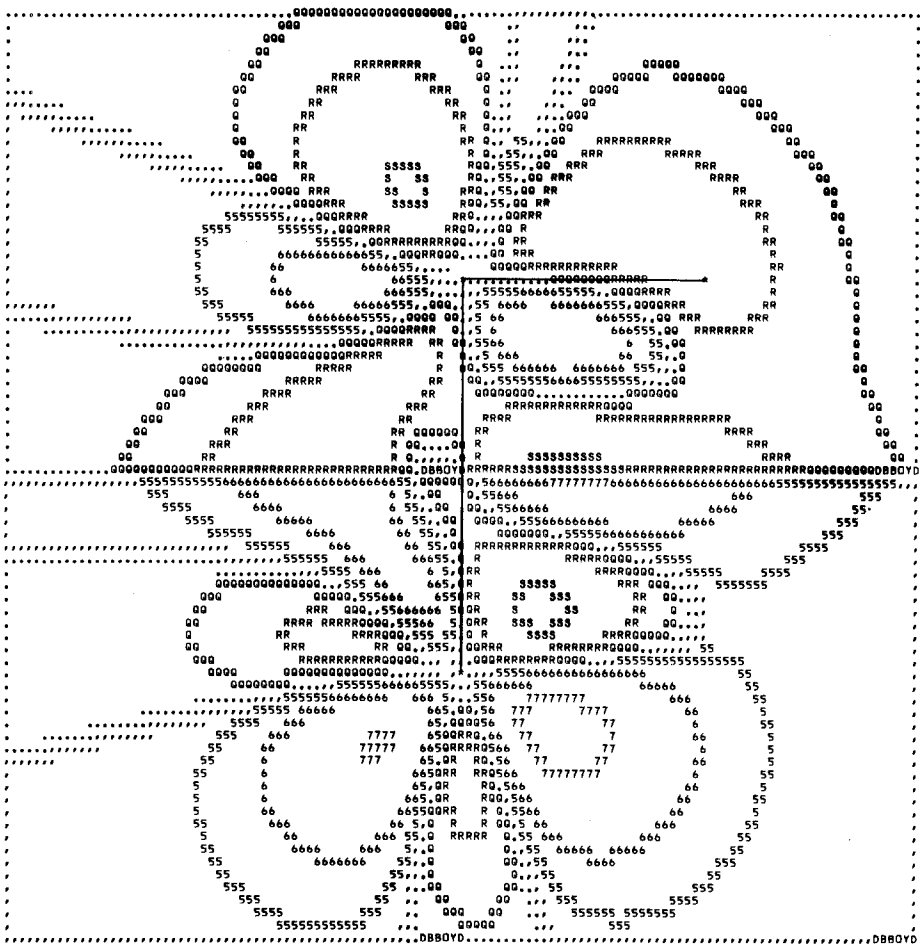

Fig. 4. Difference in the electron densities in the 90° conformer minus that in the 0° conformer. Each half shows the density in the half of the molecule where the atomic positions are fixed with respect to internal rotation, i.e., the two halves of Fig. 2 are subtracted from the upper and lower halves of Fig. 3. The features to observe are at the ends of the molecule near each S–H moiety because the redistributions along the S–S bond are partially masked by the tails of the AO's centered on the nuclei which change position

between the lone-pair clouds is increased relative to the situation in which the lone-pair regions are assumed to be pure $3p_\pi$ or sp hybrid orbitals. Compensating for the build-up of density on the obtuse side of the S–S–H angle is a loss of electrons from the other sides of the sulfur atoms. In going from the 0° to the 90° conformation, the pattern of charge redistribution is complex. The bottom half of Fig. 4 shows that in the plane perpendicular to the S–S–H group, the electrons are shifted from behind the plane of Figs. 5–7 to the side between the sulfurs. But in the plane of the S–S–H group, the electrons are shifted into the vicinity of the hydrogen (Fig. 7) and toward the ends of the S–S axis (top of Fig. 4).

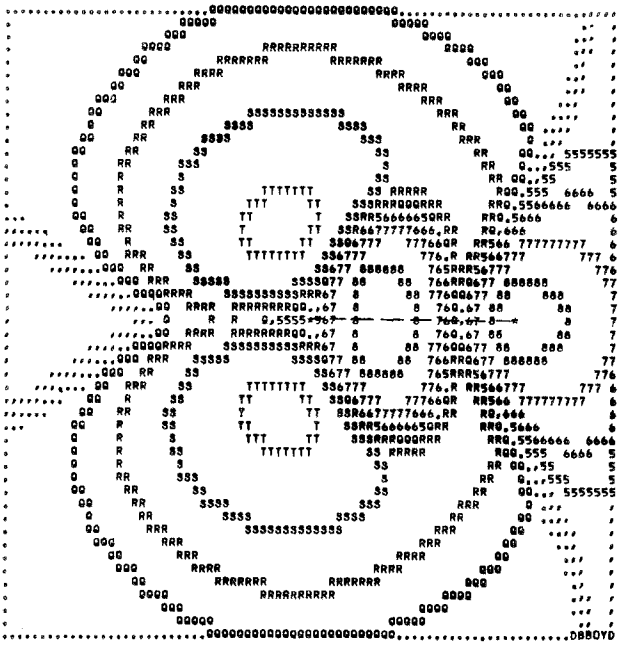

Fig. 5. Electron density in the 0° conformer of HSSH. The difference in molecular and atomic densities is computed in the plane passing through one sulfur perpendicularly to the S–S bond. Thus, one S–H bond axis lies slightly skew to this plane due to the S–S–H bond angle of ~91.5°. The map covers 4 × 4 Å

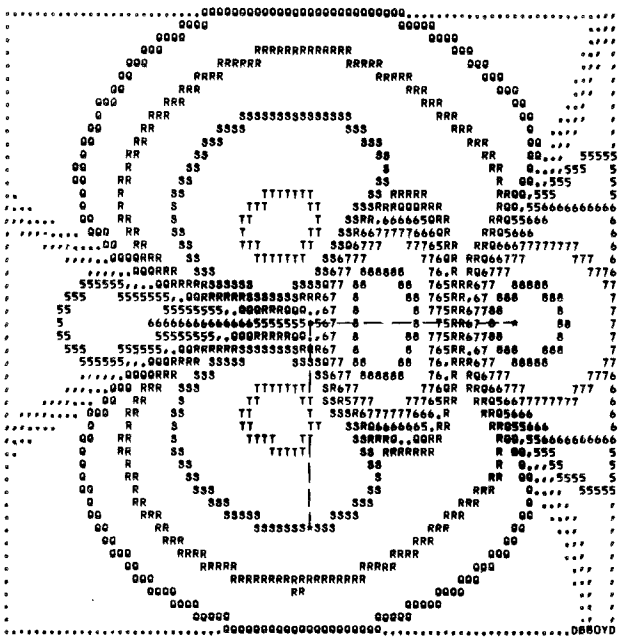

Fig. 6. Electron density in the 90° conformer of HSSH. The arrangement is like that in Fig. 5

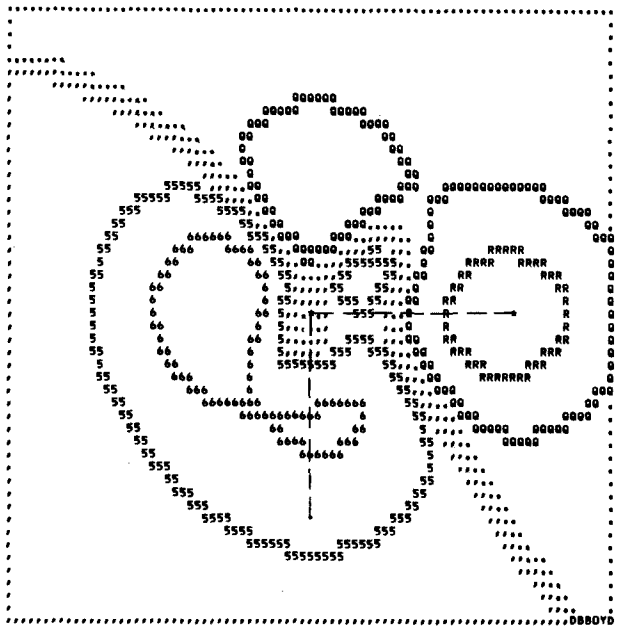

Fig. 7. Difference in the electron density in the 90° conformer of HSSH minus that in the 0° conformer. The density of Fig. 5 is subtracted from that in Fig. 6

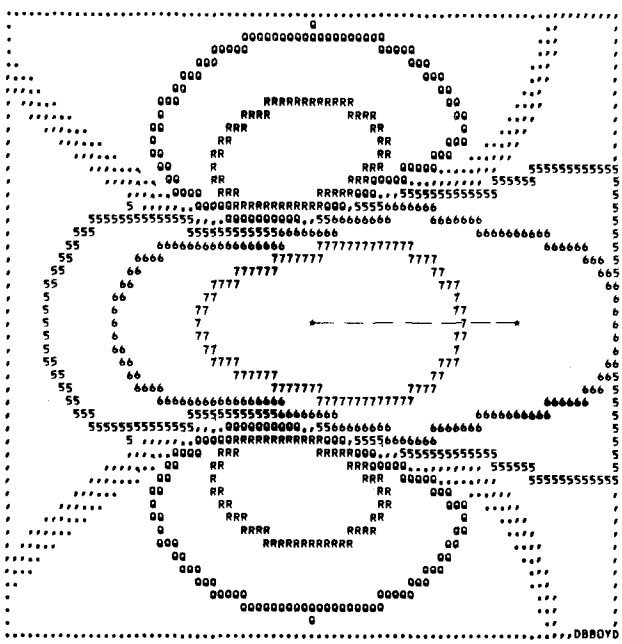

Fig. 8. Electron density in the 0° conformer of HSSH. The difference in molecular and atomic densities is shown in the plane bisecting the S–S bond perpendicularly. The map covers 4 × 4 Å

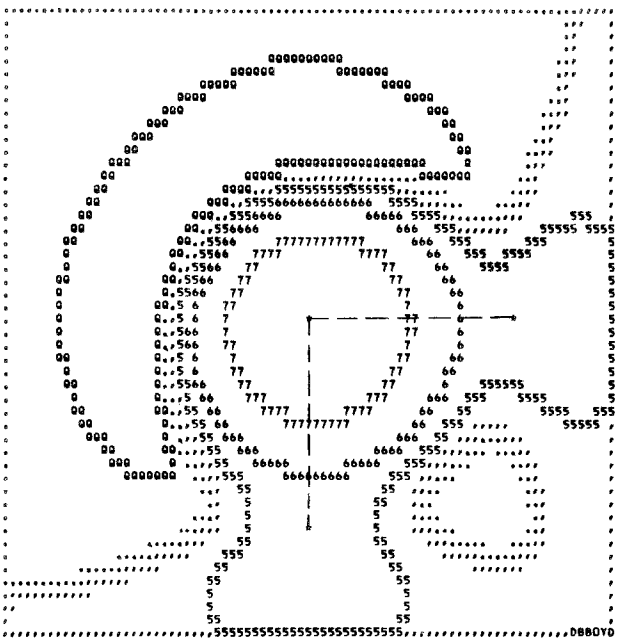

Fig. 9. Electron density in the 90° conformer of HSSH. The arrangement is like that in Fig. 8

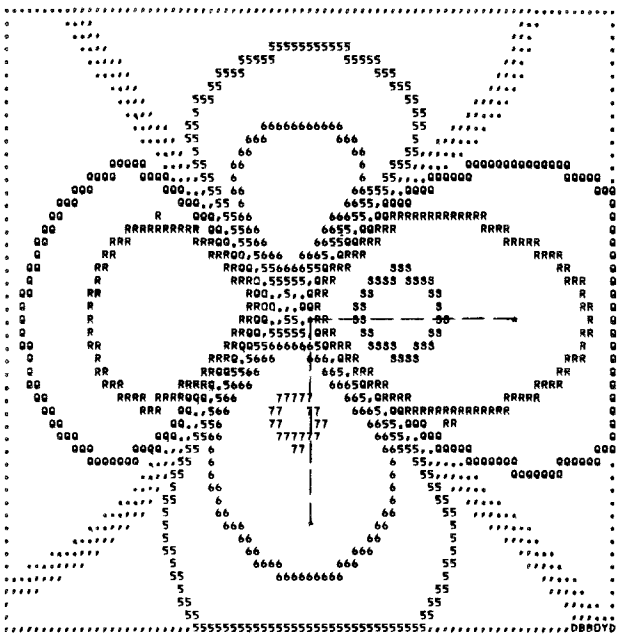

Fig. 10. Difference in the electron density in the 90° conformer of HSSH minus that in the 0° conformer. The density of Fig. 8 is subtracted from that in Fig. 9

Relative to the overlapping, but unperturbed, constituent atomic densities, the accumulation of electrons in the S–H bonds is rather small and strongly polarized away from the center of the molecule. In this respect, the S–H bond is similar to the O–H bond density obtained from all-electron wave functions [10]. Twisting the molecule from 0–90° increases the density near the hydrogens (Figs. 4 and 7). That the σ electron peak is higher in the 90° conformer is also apparent in Fig. 3 by the extra contour between sulfur and hydrogen.

The EH MO's give no density accumulation along the S–S bond expected for σ bonding (Figs. 2, 3, 8, 9). There does appear to be π bonding between the sulfurs as evidenced by the build-up of density between the sulfurs, but radially out from the S–S axis (Figs. 8 and 9). For instance, in the 90° conformer, there is a region of excess electrons (compared to the atomic densities) on the obtuse side of the dihedral angle. Comparison of the 90° and 0° conformers (Fig. 10) shows a roughly four-fold rearrangement. Visually estimating the contour sizes leads one to believe that there is a slight net increase in electron density at the midpoint of the S–S bond in the 90° conformer.

Discussion

We begin this section by distilling from our population analysis results a qualitative, intuitive model for understanding the conformational preference of a disulfide moiety. Then this model will be refined on the basis of the more detailed description provided by the electron density maps. And, finally, our model will be discussed in relation to models proposed by other authors.

The population analysis yielded the fact that the S–S overlap population is greatest when the dihedral angle is near 90°. Thus, the S–S bond is strongest when the molecule is in its equilibrium conformation. However, we also saw that there are repulsive, antibonding interactions between the S $3p_\pi$ AO's, which are highly occupied by the lone-pair electrons [1]. The S–S overlap population peaks at 90° where these repulsions are diminished. In addition, the negative net atomic charge on the sulfurs is lessened in the 90° conformation. This implies that electrons have moved away from the sulfurs toward the substituents.

The electron density maps show us exactly where the electrons are distributed around the nuclear skeleton without arbitrary partitioning of the density among the atoms or bonds. We saw that the regions occupied by the lone-pair electrons are "*C*"-shaped. In the 90° rotamer the effective distance between these regions is increased, and the interelectron repulsions are diminished. There also appears to be a slight increase in density halfway between the sulfurs as a result of twisting the dihedral angle from 0° or 180° to 90°. This migration would correlate with the increase in overlap population. Rearrangement of charge close to each sulfur nucleus is complex and difficult to interpret. On the other hand, the clear increase in density close to the hydrogen nuclei in the 90° conformer suggests a corresponding decrease in charge near the sulfurs and a more stable environment for the electrons remaining in the lone-pair clouds.

Various earlier models for understanding the conformational preference of disulfides are consistent with our calculations. Pauling [26, 27] proposed that

the repulsion of unshared electron pairs on adjacent atoms determines the orientation of the substituents about the single bond between those atoms. He assumed that the unshared electron pairs of each sulfur occupy orbitals orthogonal to each S–S–H plane, such as a $3p_\pi$ AO or an *sp* hybrid orbital. Of course, in EH MO calculations no assumptions about the hybridization of the orbitals occupied by the lone-pair electrons need be made. The electron density maps show precisely how the MO's distribute the lone-pair electrons in "*C*"-shaped regions. The "*C*"-shaped clouds act effectively like $3p_\pi$ or *sp* orbitals in that repulsive interactions between them are reduced at a dihedral angle of 90°. Another proposal for the conformational preference of disulfides is the hyperconjugation model [2]. In it, π bonding between the sulfurs is believed to be enhanced when the orbital of the unshared electron pair on one sulfur is in the same plane as the S–H bond of the other sulfur. Thus, in the 90° conformer, resonance structures of the type $H^- \; S{=}S^+{-}H$ become important. Essentially equivalent to this model is one based on a stabilizing back donation of the lone-pair electrons on one sulfur into the antibonding S–H σ^* orbital at the other end of the molecule [28]. The consequences of hyperconjugation or back donation are that the S–S bond is strengthened and the density near the hydrogens is increased in the 90° conformation. As we have seen, the EH (and *ab initio*) population analyses and the EH electron density maps support this view.

Yet another model for molecules with lone-pair electrons on adjacent atoms has been expressed as the gauche effect [29–31]. Most such molecules adopt a conformation which allows the maximum number of gauche interactions between lone-pairs and/or polar bonds, although there are a few exceptions (e.g., FCH_2OH) which must be explained by additional rules and effects [28–32]. In order to rationalize the gauche effect [29–31], Wolfe *et al.*, employed Allen's repulsive-dominant, attractive-dominant scheme [33–35] for dissecting *ab initio* total energies [15, 17]. However, characterizations based on such dissections change depending on the basis set and on whether the molecular structure is allowed to relax in the transition state [36–39]. Hence this scheme does not seem to be a dependable approach to "understanding" rotational barriers. For convenience of counting gauche interactions, Wolfe *et al.*, treated the lone-pair electrons as if they occupied sp^3-like hybrid orbitals, although they emphasized that the computed potential energy curves for internal rotation in their example of FCH_2OH [29] suggested a quasi-spherical distribution of lone-pair electrons on oxygen. Our electron density maps of HSSH show the lone-pair regions on either side of the S–S–H planes to have higher density than in the plane, but there is still an appreciable amount in the plane. In other words, our findings indicate a small amount of directionality in the spatial distribution of the two electron pairs on a divalent atom. This result is consistent with *ab initio* electron density maps of H_2S [40], computed potential energy curves for internal rotation in CH_3OH [28, 29], computed potential energy curves for hydrogen bonded systems of water [41], and electrostatic potential energy calculations of oxirane and thiirane [42]. Published [43] electron density maps of FCH_2OH have not yet dealt with the question of whether a difference density map would show a directed valence around oxygen or a distribution which is quasi-spherical like the potential field it produces [28, 29].

In summary, we have seen that new insight into the origin of the preferred conformation of disulfides can be gained by the increasingly popular expedient of mapping the electron density of EH MO's. Both published and unpublished investigations in our laboratories on a variety of phosphorus compounds, hydrocarbons, and other organic molecules have established that many chemically significant features of the electronic structures of molecules are displayed by plots of EH MO's. One may recall that EH MO's were the orbitals instrumental (even if not essential) in the development of the famous Woodward-Hoffmann rules [44]. Our spectral study [1] and the similarities of the trends in the *ab initio* and EH population analyses of HSSH encourage us to think that the EH density maps may also exhibit the important aspects of the electron redistribution, especially in our situation where comparable wave functions for different rotamers are being compared. Nevertheless, it should be kept in mind that some discrepancies between *ab initio* and EH electron density maps can be expected not only because of the semiempirical nature [13] and neglect of the core electrons [8, 40] in the EH wave functions, but also because of the different basis sets. The *ab initio* wave functions for HSSH which have been computed [15–17], but not yet published in full form, were expanded over Gaussian-type functions, whereas the EH MO's are linear combinations of Slater-type orbitals. Even different *ab initio* wave functions can yield density maps which display a modest to high dependence on the size and type of basis set [8, 40, 45–48]. Nevertheless, the very fact that several *ab initio* wave functions are available for HSSH makes our presentation of the EH results all the more worthwhile, so that at least a visual comparison can be made once the *ab initio* electron density maps are available.

Acknowledgements. Conversations with N. L. Allinger, W. A. Goddard, III, R. Hoffmann, W. N. Lipscomb, and M. M. Marsh were helpful to the development of some of the ideas in this paper.

References

1. Boyd, D. B.: J. Am. Chem. Soc. **94**, 8799 (1972).
2. Winnewisser, G., Winnewisser, M., Gordy, W.: J. Chem. Phys. **49**, 3465 (1968).
3. Sutter, D., Dreizler, H., Rudolph, H. D.: Z. Naturforsch. **20**, 1676 (1965).
4. Beagley, B., McAloon, K. T.: Trans. Faraday Soc. **67**, 3216 (1971).
5. Boyd, D. B., Lipscomb, W. N.: J. Theoret. Biol. **25**, 403 (1969).
6. Hoffmann, R., Boyd, D. B., Goldberg, S. Z.: J. Am. Chem. Soc. **92**, 3929 (1970).
7. Boyd, D. B.: J. Am. Chem. Soc. **94**, 6513 (1972).
8. Boyd, D. B.: Theoret. Chim. Acta (Berl.) **20**, 273 (1971).
9. Boyd, D. B.: J. Am. Chem. Soc. **91**, 1200 (1969).
10. Boyd, D. B.: Theoret. Chim. Acta (Berl.) **18**, 184 (1970).
11. Boyd, D. B., Hoffmann, R.: J. Am. Chem. Soc. **93**, 1064 (1971).
12. Martensson, O.: Acta Chem. Scand. **25**, 3763 (1971).
13. Boyd, D. B.: J. Am. Chem. Soc. **94**, 64 (1972).
14. Mulliken, R. S.: J. Chem. Phys. **23**, 1833 (1955).
15. Schwartz, M. E.: J. Chem. Phys. **51**, 4182 (1969).
16. Veillard, A., Demuynck, J.: Chem. Phys. Letters **4**, 476 (1970).
17. Hillier, I. H., Saunders, V. R., Wyatt, J. F.: Trans. Faraday Soc. **66**, 2665 (1970).
18. Bergson, G.: Ark. Kemi **12**, 233 (1958); **18**, 409 (1962).
19. Linderberg, J., Michl, J.: J. Am. Chem. Soc. **92**, 2619 (1970).

20. Boyd, D. B.: In: The purines: theory and experiment, Bergmann, E. D., Pullman, B. (Eds.), p. 48. Jerusalem: Israel Academy of Sciences and Humanities, 1972.
21. McClellan, A. L.: Tables of experimental dipole moments, p. 26. San Francisco, Calif.: W. H. Freeman and Co. 1963.
22. Fraser, R. R., Boussard, G., Saunders, J. K., Lambert, J. B., Mixan, C. E.: J. Am. Chem. Soc. **93**, 3822 (1971).
23. Perahia, D., Pullman, B.: Biochem. Biophys. Res. Commun. **43**, 65 (1971).
24. Ponnuswamy, P. K.: Thesis, University of Madras, India 1970.
25. Yamabe, H., Kato, H., Yonezawa, T.: Bull. Chem. Soc. Japan **44**, 604 (1971).
26. Pauling, L.: Proc. Nat. Acad. Sci. U.S. **35**, 495 (1949).
27. Pauling, L.: Nature of the chemical bond, p. 134. Ithaca, N.Y.: Cornell University Press, 1960.
28. Radom, L., Hehre, W. J., Pople, J. A.: J. Am. Chem. Soc. **94**, 2371 (1972).
29. Wolfe, S., Rauk, A., Tel, L. M., Csizmadia, I. G.: J. Chem. Soc. B, **1971**, 136.
30. Wolfe, S.: Accounts Chem. Res. **5**, 102 (1972).
31. Wolfe, S., Tel, L. M., Liang, J. H., Csizmadia, I. G.: J. Am. Chem. Soc. **94**, 1361 (1972).
32. Hine, J., Dalsin, P. D.: J. Am. Chem. Soc. **94**, 6998 (1972).
33. Fink, W. H., Allen, L. C.: J. Chem. Phys. **46**, 2261, 2276 (1967).
34. Allen, L. C.: Chem. Phys. Letters **2**, 597 (1968).
35. Jorgensen, W. L., Allen, L. C.: J. Am. Chem. Soc. **93**, 567 (1971).
36. Epstein, I. R., Lipscomb, W. N.: J. Am. Chem. Soc. **92**, 6094 (1970).
37. Veillard, A.: Theoret. Chim. Acta (Berl.) **18**, 21 (1970).
38. Clementi, E., Niessen, W. von: J. Chem. Phys. **54**, 521 (1971).
39. Lehn, J. M., Munsch, B.: Mol. Phys. **23**, 91 (1972).
40. Boyd, D. B.: J. Chem. Phys. **52**, 4846 (1970).
41. Del Bene, J. E.: J. Chem. Phys. **55**, 4633 (1971); **56**, 4923 (1972).
42. Bonaccorsi, R., Scrocco, E., Tomasi, J.: J. Chem. Phys. **52**, 5270 (1970).
43. Robb, M. A., Haines, W. J., Csizmadia, I. G.: J. Am. Chem. Soc. **95**, 42 (1973).
44. Woodward, R. B., Hoffmann, R.: The conservation of orbital symmetry. New York: Academic Press 1970.
45. Laws, E. A., Lipscomb, W. N.: Israel J. Chem. **10**, 77 (1972).
46. Kern, C. W., Karplus, M.: J. Chem. Phys. **40**, 1374 (1964).
47. Ransil, B. J., Sinai, J. J.: J. Chem. Phys. **46**, 4050 (1967).
48. Ransil, B. J., Sinai, J. J.: J. Am. Chem. Soc. **94**, 7268 (1972).

Dr. D. B. Boyd
The Lilly Research Laboratories
Eli Lilly and Company
Indianapolis, Indiana 46206, USA